JOURNAL OF Applied Polymer SCIENCE

Preparation and Properties of Aluminum Nitride-Filled Epoxy Composites: Effect of Filler Characteristics and Composite Processing Conditions

B. L. Zhu,[1] J. Wang,[1] J. Ma,[1] J. Wu,[1] K. C. Yung,[2] C. S. Xie[3]

[1]Key Laboratory for Ferrous Metallurgy and Resources Utilization of Ministry of Education, Wuhan University of Science and Technology, Wuhan 430081, People's Republic of China

[2]Department of Industrial and Systems Engineering, The Hong Kong Polytechnic University, Hung Hom, Kowloon, Hong Kong, People's Republic of China

[3]Department of Materials Science and Engineering, Huazhong University of Science and Technology, Wuhan 430074, People's Republic of China

Correspondence to: B. L. Zhu (E-mail: zhubailin97@hotmail.com)

ABSTRACT: Polymer-matrix composites based on brominated epoxy as the matrix and aluminum nitride (AlN) particle as the filler were prepared. Effects of AlN size and content as well as composite processing conditions on the preparation and properties of the composites had been investigated. At the same processing conditions, Young's modulus (E) and dielectric constant (D_k) of the composites increase, whereas coefficient of thermal expansion decreases when increasing AlN content or decreasing AlN size; tensile strength and elongation at break first increase then decrease with AlN content, and they reach maximum values at lower AlN content with decreasing AlN size; glass transition temperature (T_g) also exhibits a trend of first increase then decrease with AlN content, and it decreases with decreasing AlN size, especially at high AlN content; dissipation factor (D_f) generally decreases with AlN content except for the composites filled with 50 nm-AlN, and it increases with decreasing AlN size. Comparing the composites prepared at different processing conditions, the properties of the composite are relatively poor at low vacuum conditions during removal of solvent and bubble. The scanning electron microscope and Fourier transform infrared analyses indicate that the properties of the composites are related to the aggregation of AlN filler and voids in the composites as well as the crosslink density of epoxy matrix. The preparation of the composites is also found to be affected by AlN size and content as well as vacuum conditions, indicating that increase of viscosity of system and/or the solvent evaporation during curing results in poor formability of the composites. © 2012 Wiley Periodicals, Inc. J. Appl. Polym. Sci. 000: 000–000, 2012

KEYWORDS: AlN; epoxy-matrix composites; thermal properties; dielectric properties; tensile properties; microstructure; crosslink density; viscosity; nanometer-sized filler

Received 29 August 2011; accepted 28 February 2012; published online 00 Month 2012
DOI: 10.1002/app.37599

INTRODUCTION

Thermal conductivity is increasingly important for electronic packaging and/or substrate materials because the heat dissipation ability limits the reliability, performance, and miniaturization of electronics.[1] In addition to high thermal conductivity, high electrical resistivity and a low coefficient of thermal expansion (CTE) are needed for resistance to thermal fatigue.[2] The dielectric properties of the electrical packaging and/or substrate materials, including the dielectric constant (D_k) and dissipation factor (D_f), play a very important role in signal conveying as the working frequency of electronic appliances increases. Low D_k and D_f are demanded for packaging and/or substrate materials in high-frequency appliance markets to increase the velocity of signal propagation.[3] In addition, necessary mechanical properties are also required for electrical packaging and/or substrate materials. In a word, the materials used for electrical packaging and/or substrate need to have more multifunctional properties, such as excellent thermal, dielectric, and mechanical properties at the same time, including high thermal conductivity, glass transition temperature (T_g), and tensile strength and low CTE, D_k, and D_f.

Up to now, a sole polymer material is hard to satisfy the demand for above multifunctional properties because of its high CTE and

low thermal conductivity. To offset these deficiencies, adding inorganic particles to a polymer is a versatile method. Different fillers including oxide, carbide, nitride, and carbon materials have been investigated.[4–8] Among these fillers, aluminum nitride (AlN) has been considered as an ideal candidate owing to its very high thermal conductivity, no toxicity, stable crystal structure, and relatively low cost. Thus, AlN-filled polymer-matrix composites are potentially used as the primary materials for electrical packaging and/or substrate materials. Many researches have observed that the thermal conductivity can be significantly increased in different polymer–AlN composites,[4–12] and other properties such as CTE, tensile strength, and D_k of polymer can also be modified by adding AlN.[4,5,9,10,13–17] However, there is lacking a systematical investigation of the effect of AlN size and content on the thermal, dielectric, and mechanical properties of the composite as well as its preparation. On the other hand, the effect of composite processing conditions on the preparation and properties was seldom considered in previous reports. In fact, it was reported that solvent used in preparing composites could affect the curing kinetics and mechanism of the epoxy/dicyandiamide (DICY) system in addition to the DICY-to-epoxy ratio and curing temperature and time. Comparing the solvents used in the fabrications of composite, it was found that the species would be preferably absorbed on the surfaces of fillers and the reaction of DICY with the epoxy was changed owing to the differences in solubility of constituents in various solvents.[18,19] Moreover, the solvent evaporation during curing at high temperature will generate voids in the cured resin. Hence, the composite processing conditions, especially the removal of solvent, affect the preparation and properties of the composites. Obviously, the composite processing conditions are linked to the filler size and content. Usually, high-performance composites are obtained by changing filler size and content. However, the viscosity of system changes with variation in filler size and content, which will affect the removal of solvent, dispersion of filler, and curing mechanism of epoxy, and thus the preparation and properties of the composites are modified.

In the present study, we change the AlN size and content at the same processing condition or change the processing condition at the same AlN size and content to evaluate the effect of filler characteristics and processing condition over the preparation and properties of the composites. Our results showed that the effects of AlN size and content as well as composite processing condition finally exhibited to change the formability, microstructure of the composites, and crosslink density of the epoxy matrix, and thus the preparation and properties of the composites were affected by AlN characteristics and processing conditions.

EXPERIMENTAL PROCEDURE

Raw Materials

Three kinds of AlN powders were purchased from Hefei Kiln Nanometer Technology Development (Heifei, China) with average sizes being about 2.3 μm, 0.5 μm, and 50 nm, and they were denoted as 2.3 μm-AlN, 0.5 μm-AlN, and 50 nm-AlN, respectively. The coupling agent was 3-glycidoxypropyltrimethoxysilane (trade name KBM-403), purchased from Shin-Etsu Handotai (SEH, Tokyo, Japan). The epoxies used as the matrix were Epon 8008 and Epon 1031, purchased from Huntsman (Salt Lake City, Utah). Epon 8008 is a kind of brominated epoxy resin that has been specially designed to meet the stringent requirements of the printed circuit board industry. It has an epoxide equivalent of 410–460 g/Eq, and a bromine content of 19.0–21.0% w/w. Epon 1031 is a solid multifunctional epichlorohydrin/tetraphenylol ethane epoxy resin with an epoxy group content of 4350–5130 mmol/kg. Epon 1031 is used to improve the properties of cured epoxy resin systems, particularly at elevated temperatures. In this study, Epon 8008 and Epon 1301 have been dissolved in acetone, and their contents in the solution are 80 and 70% w/w, respectively. The curing agent DICY (purity, >99.5%) and the accelerator 2-methylimidazole (2-MI, purity, >99.0%) were obtained from Neuto Products (Taipei, Taiwan) and Tokyo Kasei Kogyo (Tokyo, Japan), respectively. The DICY particles had an average diameter of <1 mm. DICY and 2-MI were used as received.

Table I. Basic Recipe of Epoxy Resin–AlN Composite

Materials	Ratio of materials by weight
Epon 8008 solution	100
Epon 1301 solution	7.349
DICY	2.552
2-MI	0.056
AlN	0–160

Procedure for Composite Preparation

The epoxy–AlN composites were fabricated according to the following steps: (i) the surface of the AlN powder was pretreated with KBM-403 coupling agent, with the amount used being 5 wt% based on the weight of the AlN powder; (ii) Epon 8008 solution, Epon 1031 solution, DICY, 2-MI, and AlN were weighed at a certain ratio as listed in Table I; (iii) the mixtures, further diluted by acetone, were first stirred in a beaker for 45 min by an ultrasonic stirrer, and then they were stirred by a high-speed mixing machine for 1 h; (iv) the uniformly formed mixtures were cast in a mold and were pumped for about 1 h in vacuum dry oven to remove the air bubbles and solvent as the temperature gradually increased from 80 to 130°C; and (v) finally, they were heated to 175°C for 4 h to complete polymerization.

When the weight ratio of AlN to Epon 8008 solution (W_{f-E}) varied from 2.5 to 40%, single 50 nm-AlN powders were first chosen. Considering that the properties of the composites are also affected by size distribution of filler, mixed fillers of 2.3 μm-AlN and 50 nm-AlN with a simple and typical weight ratio of 1 : 1 (denoted as 2.3 μm + 50 nmAlN) were used. When W_{f-E} varied from 2.5 to 160%, 2.3 μm-AlN-filled composites were prepared. When W_{f-E} varied from 10 to 80%, mixed fillers of 2.3 μm-AlN and 0.5 μm-AlN with weight ratio of 3 : 1 (denoted as 2.3 + 0.5 μmAlN) was used. During preparation of above samples, the gas pressure in oven was decreased to about 100 Pa (high vacuum) by mechanical vacuum pump during removal of solvent and bubble. When W_{f-E} are 60–160 and 10–80%, 2.3 μm-AlN and 2.3 + 0.5 μm-AlN filled composites were also prepared at gas pressure in the oven of about 2000 Pa (low vacuum), respectively.

Characterization

Filler Volume Fraction. The volume percent of AlN filler in the composites was determined using the following equation:

$$V_f = \frac{\frac{W_{f-E}}{0.877523 + W_{f-E}}}{\frac{W_{f-E}}{0.877523 + W_{f-E}} + \left(1 - \frac{W_{f-E}}{0.877523 + W_{f-E}}\right) \bullet \frac{\rho_f}{\rho_m}} \quad (1)$$

where W_{f-E} is the weight ratio of AlN to Epon 8008 solution, as mentioned above; $W_{f-E}/(W_{f-E} + 0.877523)$ is the weight fraction of AlN filler in the composite samples (W_f) according to the recipe listed in Table I; ρ_f and ρ_m are the densities of the fillers (3.26 g/cm^3) and pure epoxy (1.3846 g/cm^3), respectively. The obtained volume fraction of AlN in the composites varied from 0 to 43.64%.

Tensile Properties Test. The tensile properties of the composites were measured by using a hydraulic mechanical testing system (MTS 812) at a crosshead speed of 0.5 mm/min. The strain was measured by a strain gauge (D 638-03). The values of Young's modulus (E), tensile strength, and elongation at break are the average values of at least three samples.

CTE and T_g Measurement. The CTE and T_g of the composites were measured with a Perkin-Elmer thermal mechanical analyzer (TMA-7). The temperature range used was from 30 to 220°C, and the heating rate was 10°C/min. All reported TMA data were obtained from a second heating cycle, and at least four samples were tested for each composite formulation.

Dielectric Properties Measurement. D_k and D_f measurements were taken on an Agilent-4294A impedance analyzer with an applied AC voltage of 500 mV and frequency range of 1 KHz–1 MHz. The used samples were disk shaped, and both sides of the samples were coated with silver paste. The D_k was calculated from capacitance (C) by $D_k = Ct/\varepsilon_0 A$, where t was the thickness of the disk, ε_0 the vacuum dielectric constant, and A the disk area. For each composite formulation, a minimum of five specimens were tested, and the average values of D_k and D_f were reported in the article.

Thermal Conductivity Measurement. The thermal conductivity was given by the product of the thermal diffusivity, specific heat, and density. The thermal diffusivity and specific heat of the composites were measured by Flashline™ 3000 Thermal Properties Analyzer (Anter Pittsburgh, Pennsylvania (PA)). The samples were disk shaped with 12.7 mm diameter and 0.8–1.2 mm thickness. Finally, thermal conductivity was calculated from the measured values of thermal diffusivity and specific heat capacity, with the additional knowledge of density. Thermal conductivity tests were performed using at least three specimens of each composition and the average results obtained are reported in the article.

Scanning Electron Microscope Analysis. A scanning electron microscope (SEM, Leica Stereoscan 440) and a field emission scanning electron microscope (FE-SEM, JEOL, JSM-6335F) were used to analyze the fractured surfaces of composites. A thin section of the fractured surface was mounted on an aluminum stub using a conductive (silver) paint and was coated with gold prior to fractographic examination.

Table II. The Young's Modulus (E), Tensile Strength, and Elongation at Break of the Composites Prepared at Different AlN Sizes and Contents

AlN filler size and content		Tensile properties		
Size	Content (vol %)	Young's modulus (GPa)	Tensile strength (MPa)	Elongation at break (%)
Neat epoxy	-	3.22	54.93	2.75
2.3 μm	1.2	3.27	55.17	2.76
	2.36	3.36	65.72	3.29
	4.62	3.62	76.59	3.83
	8.83	3.86	65.55	3.28
	16.22	4.48	61.01	3.05
50 nm	1.2	3.35	73.45	3.6
	2.36	3.55	55.36	1.98
	4.62	4.05	53.09	1.54
2.3 μm + 50 nm	1.2	3.28	67.13	4.43
	2.36	3.57	76.74	2.25
	4.62	4.01	60.92	2.0

Fourier Transform Infrared Analysis. Infrared absorption spectra of the composites were measured using a Fourier transform infrared (FTIR) spectrometer (Bio-Rad, Hercules, California (CA) Model: FTS 6000). KBr pellet technique was employed with resolution of 4 cm^{-1}. The dry KBr was mixed with the composites by grinding for homogenization. The fine powder was then pressed into a transparent, thin pellet. These thin pellets were used for the normal IR spectral measurements.

EXPERIMENTAL RESULTS

Mechanical Properties

The E, tensile strength, and elongation at break of the composites prepared at different AlN sizes and contents are summarized in Table II. It is observed that the E of pure epoxy is 3.22 GPa, and it increases continuously to 4.48 and 4.05 GPa at 16.22 vol % 2.3 μm-AlN, and 4.62 vol % 50 nm-AlN, respectively. At the same AlN content, the E of 50 nm-AlN-filled composite is obviously higher than that of 2.3 μm-AlN-filled composites. When 2.3 μm + 50 nm-AlN is used as filler, E of the composites is close to that of 50 nm-AlN-filled composites.

As summarized in Table II, the tensile strength of pure epoxy is 54.93 MPa, and it first increases then decreases with addition of AlN to the epoxy matrix. Maximum tensile strengths of 73.45, 76.74, and 76.59 MPa are reached at loading level of 1.2, 2.36, and 4.62 vol % for 50 nm-AlN, 2.3 μm + 50 nm-AlN, and 2.3 μm-AlN, respectively.

As summarized in Table II, the elongation at break of pure epoxy is 2.75%. When 50 nm-AlN and 2.3 μm + 50 nm-AlN are used as filler, the elongation at break increases to 3.6 and 4.43% with AlN content increasing to 1.2 vol %, and then it steeply decreases to 1.54 and 2% with AlN content further increasing to 4.62 vol %, respectively. Using 2.3 μm-AlN as filler, the

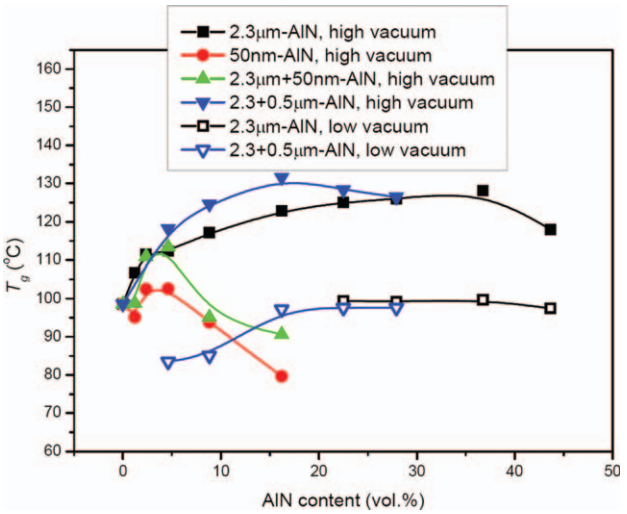

Figure 1. T_g of the composites as a function of AlN content. [Color figure can be viewed in the online issue, which is available at wileyonlinelibrary.com.]

elongation at break first increases to 3.83% as AlN content increases to 4.62 vol %, and then it decreases to 3.05% as AlN content further increases to 16.22 vol %.

***T_g* and CTE.** Figure 1 shows T_g from the TMA of the composites as a function of AlN content. The T_g of pure epoxy is 98°C. With increasing AlN content, the changed trend of T_g for the 50 nm-AlN and 2.3 μm + 50 nm-AlN-filled composites is same, that is T_g first increases to 102 and 113°C at AlN content of 4.62 vol % then greatly decreases to 80 and 90°C with further increasing AlN content to 16.22 vol %, respectively. At all AlN contents, the T_g of 2.3 μm + 50 nm-AlN-filled composites is always higher than that of 50 nm-AlN-filled composites. It is observed that T_g of the composites filled with 2.3 μm-AlN and 2.3 + 0.5 μm-AlN show a trend of first increase then slight decrease with AlN content, and maximum T_g of 128 and 132°C are obtained at AlN content of 36.74 and 16.22 vol %, respectively. When AlN content above 4.62 vol %, the T_g the composites filled with 2.3 μm-AlN or 2.3 + 0.5 μm-AlN is obviously higher than that of the composites filled with 2.3 μm + 50 nm-AlN. At low vacuum conditions, the T_g of the composites filled with 2.3 μm-AlN keeps at about 99°C at AlN content of 22.51–43.64 vol %; it increases from 83 to 98°C as AlN content increasing from 4.62 to 27.91 vol % for the composites filled with 2.3 + 0.5 μm-AlN. Obviously, the T_g of the samples prepared at low vacuum is lower than that at high vacuum regardless of 2.3 μm-AlN or 2.3 + 0.5 μm-AlN-filled composites.

Figure 2(a) shows that the CTE of pre-T_g of the composite varies with AlN content. The CTE of pure epoxy is 62.83 ppm/°C, and it obviously decreases as the AlN filler content increases, but the decreased extent depends on the AlN size and content. At the same AlN content and high vacuum condition, the CTE of the composites filled with 50 nm-AlN and 2.3 μm + 50 nm-AlN is close and is smaller than that of 2.3 + 0.5 μm-AlN and 2.3 μm-AlN-filled composites; the CTE of 2.3 μm-AlN-filled composites is slightly higher than that of 2.3 + 0.5 μm-AlN-filled composites. As AlN content increasing to 16.22, 27.91, and 43.64 vol %, the CTE decreases to 41, 35, and 26.72 ppm/°C for 50 nm-AlN (or 2.3 μm + 50 nm-AlN), 2.3 + 0.5 μm-AlN, and 2.3 μm-AlN-filled composites, respectively. At low vacuum conditions, the CTE of the composites filled with 2.3 + 0.5 μm-AlN and 2.3 μm-AlN decreases only to 43.14 and 38.03 ppm/°C at AlN content of 27.91 and 43.64 vol %, respectively. Hence, the CTE of the composites prepared at low vacuum is obviously higher than that prepared at high vacuum at the same AlN content and size.

Figure 2(b) shows the CTE of post-T_g of the composite as a function of AlN content. It is observed that the CTE of the composites shows a trend of 50 nm-AlN < 2.3 μm + 50 nm-AlN < 2.3 + 0.5 μm-AlN < 2.3 μm-AlN at the same AlN content. The CTE of pure epoxy is 217.55 ppm/°C, it decreases to 160, 132.15, and 94 ppm/°C for the composites filled with 16.22 vol % 50 nm-AlN (or 2.3 μm + 50 nm-AlN), 27.91 vol % 2.3 + 0.5 μm-AlN, and 43.64 vol % 2.3 μm-AlN, respectively. Also, the CET of post-T_g of the composite prepared at low vacuum is higher than that at high vacuum, which is indicated by that the CTE decreases only to 141.35 and 104.55 ppm/°C at 27.91 vol % 2.3 + 0.5 μm-AlN and 43.64 vol % 2.3 μm-AlN, respectively. All in all, the dependence of CTE of post-T_g on AlN size and content as well as composite processing condition is similar to that of pre-T_g, that is, smaller filler size, high loading level, and high vacuum condition are beneficial to decrease the CTE of the composites.

Dielectric Properties

The curves of D_k and D_f versus the frequency from 10^3 to 10^6 Hz for typical composites are shown in Figure 3. It is observed

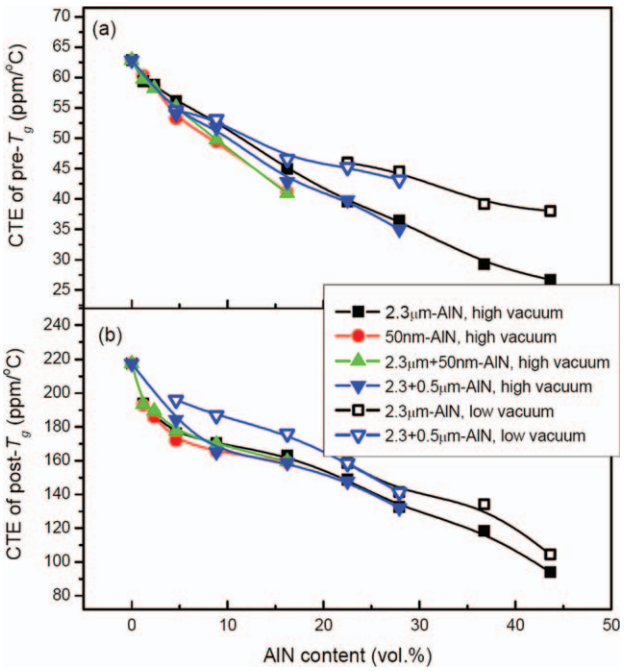

Figure 2. CTE before T_g (a) and after T_g (b) as a function of AlN content. [Color figure can be viewed in the online issue, which is available at wileyonlinelibrary.com.]

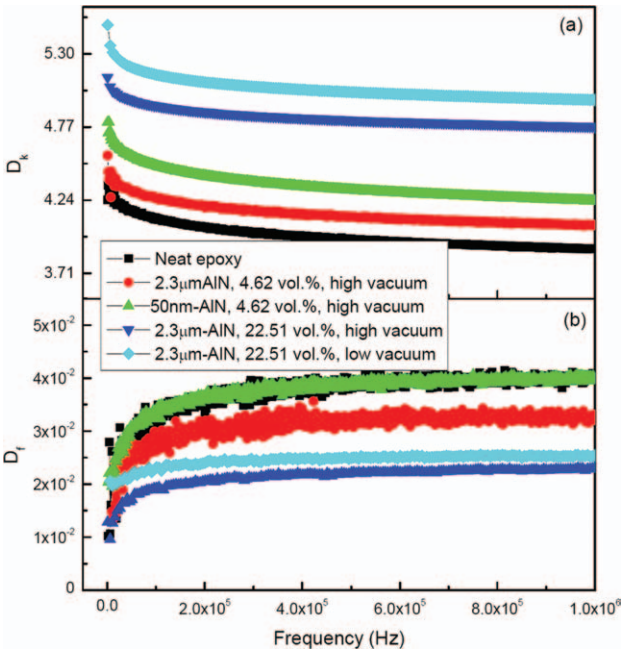

Figure 3. The D_k (a) and D_f (b) of typical composites as a function of testing frequency. [Color figure can be viewed in the online issue, which is available at wileyonlinelibrary.com.]

that the D_k decreases but the D_f increases with increasing frequency for all the samples. The dielectric properties of material are determined by its polarizabilities. There are four major types of polarizations with their polarization relaxations occurring at specific frequencies[20]: electronic or ionic displacement polarization (10^{12}–10^{15} Hz), electronic or ionic relaxation polarization (10^{2}–10^{10} Hz), molecular or dipolar polarization (10^{2}–10^{10} Hz), and interfacial polarization (around 1–10^{-3} Hz). In the present study, frequency of applied electric field (f) is 10^{3}–10^{6} Hz, which implies that the electronic, ionic, molecular, or dipolar relaxation polarization mechanism may be contributed to dielectric properties of the composites, but interfacial polarization mechanism will be dramatically reduced because this polarization is too slow to completely follow the oscillation of the applied electric field. For the AlN-filled epoxy-matrix composites, molecular polarization appears at AlN filler and epoxy matrix. According to the reports, the main relaxation process of epoxy resin is α-, β-, and γ-relaxations.[21] The α-relaxation is dependent on the random motion of whole molecular, and thus it takes place at low frequencies. The β-relaxation has been attributed to the hydroxyl motion, but it provides a negligible contribution to the relaxation processes because of low concentration of hydroxyl group in the system. The γ-relaxation is the motion of dipolar groups of atoms, which should include epoxy and amine groups with the unreacted diglycidyl ether of bisphenol-A (DGEBA) and DICY and dipolar groups with intermediate products and final polymer. At low frequencies, the molecular polarization will have more time to complete compared with that at high frequencies. Thus, the degree of polarization of composites is high and the dissipation of polarization is low at low frequencies. This reveals that the D_k decreases but the D_f increases with increasing frequency.

In Figure 4(a), the D_k at 1 MHz of the composite as a function of the AlN content is shown. It is found that the D_k of the composites increases with increasing AlN content. As increasing AlN content from 0 to 16.22 vol %, the D_k of the 50 nm-AlN and 2.3 μm + 50 nm-AlN-filled composites increases from 3.886 to 5.027 and 4.738, respectively. For the 2.3 + 0.5 μm-AlN and 2.3 μm-AlN-filled composites, the D_k increases to 4.933 and 5.32 as increasing AlN content to 27.91 and 36.74 vol %, respectively. At the same AlN content and high vacuum condition, the order of D_k of the composites is 50 nm-AlN > 2.3 μm + 50 nm-AlN > 2.3 + 0.5 μm-AlN > 2.3 μm-AlN. At the same AlN content and size, the D_k of composites prepared at low vacuum is obviously higher than that at high vacuum, for example, the D_k increases to 5.064 and 5.415 at 27.91 vol % 2.3 + 0.5 μm-AlN and 36.74 vol % 2.3 μm-AlN, respectively.

The D_f at 1 MHz of the composite as a function of AlN content is shown in Figure 4(b). Basically, monotonic decreased trend of D_f with AlN content is observed in the composites except for 50 nm-AlN and 2.3 μm + 50 nm-AlN-filled composites. Compared with D_f of pure epoxy of 0.040, D_f decreases to 0.019 and 0.024 as 2.3 μm-AlN and 2.3 + 0.5 μm-AlN content are increased to 36.74 and 27.91 vol %, respectively. The D_f of 50 nm-AlN-filled composites slightly decreases to 0.037 with increasing the AlN content to 2.36 vol %, and then it gradually increases to 0.045 with further increasing AlN content to 16.22 vol %. For the 2.3 μm + 50 nm-AlN-filled composites, the D_f slightly increases to 0.042 at 1.2 vol % AlN, thereafter it decreases to 0.035 at 16.22 vol % AlN. At low vacuum conditions, the decreased degree of D_f at the same AlN content is smaller than that at high vacuum, for example, 36.74 vol % 2.3 μm-AlN and 27.91 vol % 2.3 μm + 50 nm only decrease D_f of the composites to 0.022 and 0.026, respectively.

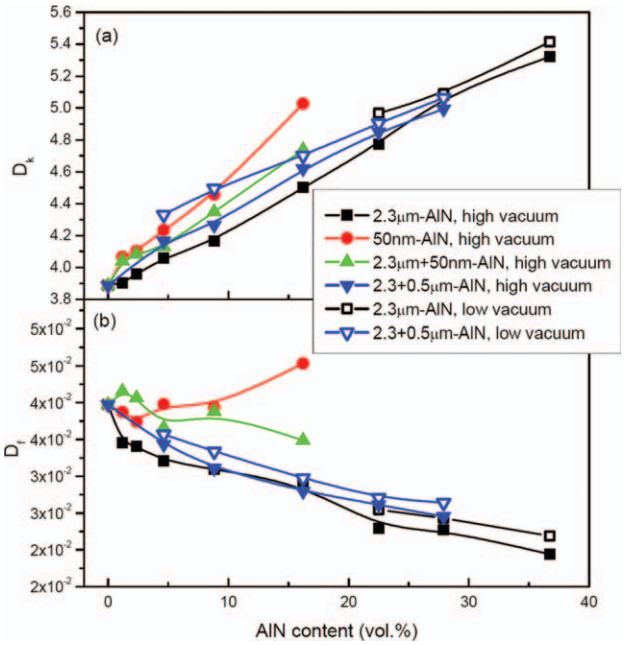

Figure 4. The D_k (a) and D_f (b) of the composites as a function of AlN content. [Color figure can be viewed in the online issue, which is available at wileyonlinelibrary.com.]

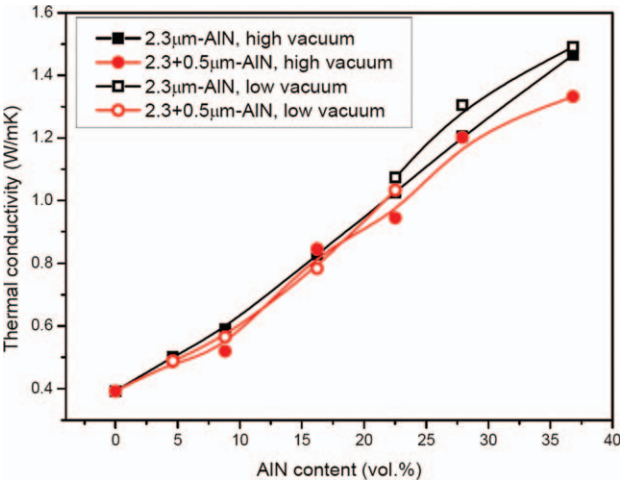

Figure 5. The thermal conductivity of the composites as a function of AlN content. [Color figure can be viewed in the online issue, which is available at wileyonlinelibrary.com.]

Thermal Conductivity

The thermal conductivity of the composite is plotted in Figure 5 as a function of AlN content. As shown in Figure 5, the thermal conductivity of the composites can be increased from 0.4 to 1.46 W/m·K as AlN content increases from 0 to 36.74 vol %. It seems that AlN size has no obvious effect on the thermal conductivity of the composites. Comparing the composites prepared at different processing conditions, the 2.3 μm-AlN-filled composites prepared at low vacuum have higher thermal conductivity than that prepared at high vacuum.

DISCUSSION

Usually, the properties of the composites are dependent on the characteristics of the matrix and filler. Owing to higher E, D_k, and thermal conductivity of AlN than those of epoxy, the E, D_k, and thermal conductivity should be increased after filling AlN into epoxy. On the contrary, the D_f and CTE of AlN are smaller than those of epoxy, and thus these properties should be decreased after filling AlN into epoxy. Considering the existence of interaction between the AlN filler and the epoxy matrix, interfacial areas between them play an important role. Supporting that AlN uniformly disperses into epoxy matrix, the interaction between AlN and matrix enhances because of the increase in interfacial areas between them as AlN content increases or AlN size decreases. Thus, we can observe that the E, D_k of the composites increase but the CTE and D_f decrease with increasing AlN content or decreasing the AlN size. However, some properties of the composites show different changed trends with AlN content. For example, the tensile strength and T_g exhibit parabolic change with AlN content; the D_f first decreases then increases with increasing 50 nm-AlN content, as mentioned above. All the properties of the composites prepared at low vacuum condition are degenerated. These results reflect that the properties of the composites are related to other factors. One main factor should be microstructure of composites.

To analyze the microstructure of the composites, we first observe the fractured surfaces of specimens at low magnification as shown in Figure 6. It is found that the fractured micrograph of neat epoxy in Figure 6(a) exhibits a smooth surface, which is a feature of typical brittle failure, thus accounting for the low toughness and strength of the unfilled epoxy. The fractured surfaces gradually become rough as 2.3 μm-AlN content increasing from 1.2 to 16.22 vol % [Figure 6(b–d)]. The increased surface roughness implies that the path of the crack tip is distorted because of the filler, making crack propagation more difficult.[22,23] Compared with 2.3 μm-AlN-filled composites, obviously increased surface roughness is observed at 50 nm-AlN-filled composites owing to smaller size even at very low content (1.2 vol %) as shown in Figure 6(e). However, when the 50 nm-AlN content further increases to 4.62 vol %, surface roughness seems to decrease [Figure 6(f)]. From the surface roughness of fractured samples, we can roughly explain the tensile stress and elongation at break increase with an addition of AlN. However, we cannot explain the decrease in the tensile stress and elongation at break with further increasing AlN content; the change of other properties of the composites with AlN size and processing conditions also cannot be explained. Thus, we further analyze the distribution state of AlN in the composites and the interface state between epoxy and AlN by FE-SEM.

Figure 7 shows FE-SEM images of fractured surface of the AlN-filled composites at different preparation conditions. The SEM images of 27.91 vol % 2.3 μm-AlN and 2.3 + 0.5 μm-AlN-filled composite prepared at high vacuum are shown in Figure 7(a,b). We can observe that the AlN surface is partly coated by epoxy and has a strong interfacial adhesion between them (marked by straight arrow). In addition, few AlN filler obviously expose on the surface and thus it is difficult to distinguish AlN filler and epoxy matrix although the AlN content reaches 27.91 vol %. This also indicates a good compatibility and strong interaction between AlN and epoxy, and thus it is difficult to peel off the AlN from epoxy matrix. The interaction between AlN and epoxy can effectively inhibit the mobility of epoxy chain, and this effect is enhanced with increasing the AlN content.[24,25] Thus, the T_g gradually increases with increasing the 2.3 μm-AlN or 2.3 + 0.5 μm-AlN content. As shown in Figure 7(a,b), agglomerations of AlN (marked by ellipse) and part separation (marked by dashed arrows) between AlN and epoxy matrix can also be observed. This implies that some weak interaction regions exist in the composite with increasing AlN content, which results in slight decrease in T_g at higher 2.3 μm-AlN or 2.3 + 0.5 μm-AlN content. Owing to high stress concentration at agglomeration regions under tensile loading, the cracks will be easily induced at the interface of the filler and polymer matrix.[22,23] Thus, the samples with 2.3 μm-AlN content higher than 4.62 vol % fail at a relatively low stress level.

For nano-AlN-filled composites, we can find that the AlN exposed on the surface form aggregation and some voids are seen in these aggregations of nano-AlN as shown in Figure 7(c–f). The aggregation of nanofiller easily forms in the composites owing to difficulty of dispersing the nanofiller. With increasing nanofiller content, the dispersion becomes more difficult because viscosity of the mixture greatly increases.[26,27] The voids originate from air bubbles and/or solvent evaporation. Although the mixture was pumped for a long time to remove the air bubbles and

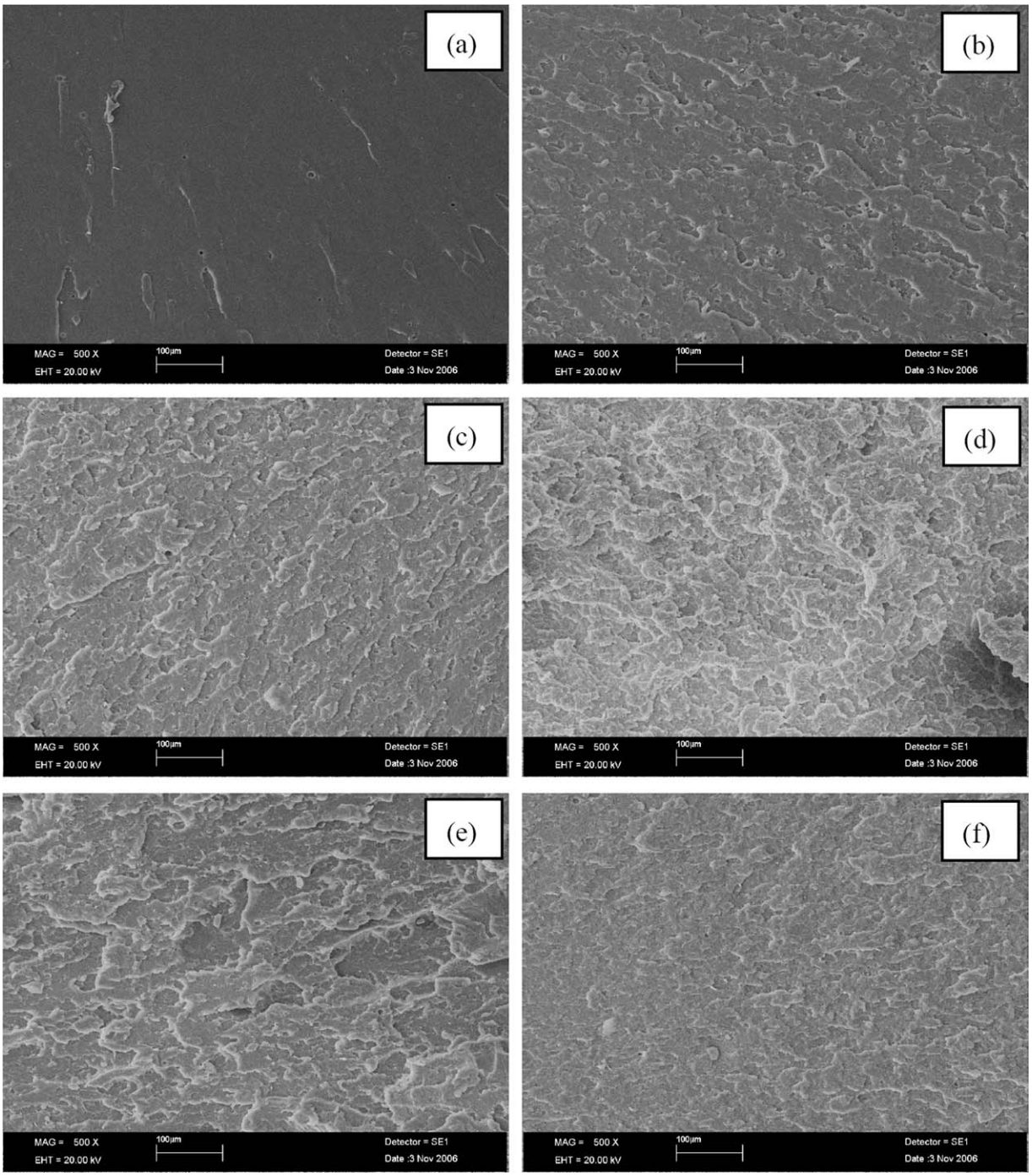

Figure 6. The SEM images of fractured surface of the composites prepared at high vacuum conditions: (a) neat; (b) 2.3 μm-AlN, 1.2 vol %; (c) 2.3 μm-AlN, 4.62 vol %; (d) 2.3 μm-AlN, 16.22 vol %; (e) 50 nm-AlN, 1.2 vol %; (f) 50 nm-AlN, 4.62 vol %.

solvent at high vacuum during the preparation of samples, it seems to be difficult to completely remove the bubbles and solvent because viscosity of the mixture gradually increases with adding 50 nm-AlN filler. The aggregation of the nanofiller and poor compatibility with the polymer also easily induce the voids appearing in the composites. Obviously, the interaction between these aggregations of 50 nm-AlN and epoxy matrix is relatively poor. Thus, the T_g of the composite containing 50 nm-AlN is smaller than that of 2.3 μm-AlN-filled composites.

As for the change in interaction between filler and epoxy matrix with filler content, we can further analyze from Figure 7(c–e), which show the SEM image of composites filled with 1.2–16.22 vol % 50 nm-AlN. At the AlN content of 1.2 and 4.62 vol %, the aggregation of 50 nm-AlN and voids are observed at local regions on the fractured surface. However, as increasing 50 nm-AlN content to 16.22 vol %, more aggregations and voids are observed at whole fractured surface as shown in Figure 7(e), which implies that the interaction and/or the interfacial

Applied Polymer SCIENCE

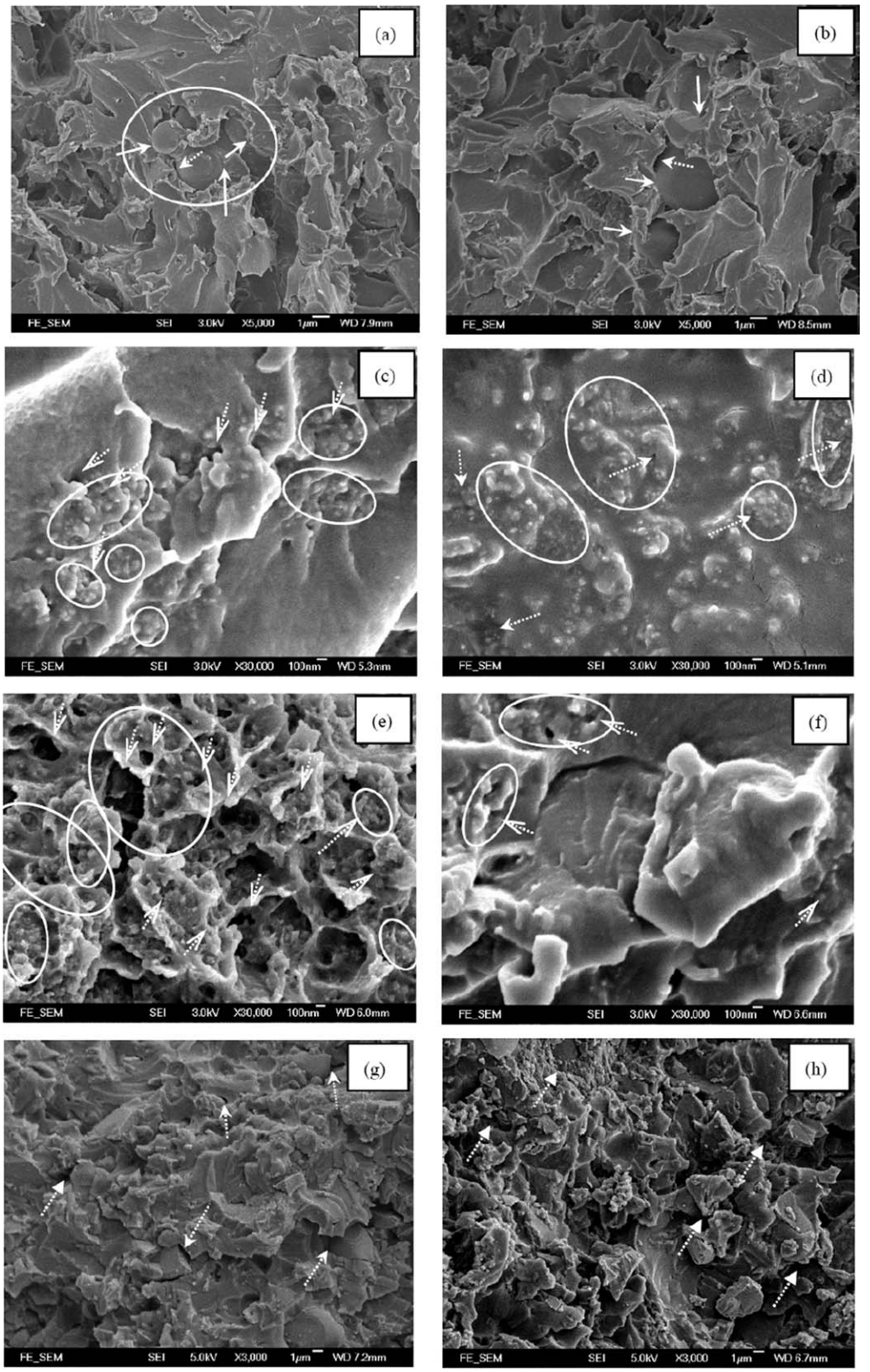

Figure 7. The FE-SEM images of fractured surface of the composites: (a) 2.3 μm-AlN, 27.91 vol %, high vacuum; (b) 2.3 + 0.5 μm-AlN, 27.91 vol %, high vacuum; (c) 50 nm-AlN, 1.2 vol %, high vacuum; (d) 50 nm-AlN, 4.62 vol %, high vacuum; (e) 50 nm-AlN, 16.22 vol %, high vacuum; (f) 2.3 μm + 50 nm-AlN, 4.62 vol %, high vacuum; (g) 2.3 + 0.5 μm-AlN, 27.91 vol %, low vacuum; (h) 2.3 μm-AlN, 27.91 vol %, low vacuum. (The contact regions between filler and epoxy are marked by straight arrows, the aggregations of filler are marked by ellipses, and the voids and/or gaps between filler and epoxy are marked by the dashed arrows.)

adhesion between 50 nm-AlN and epoxy matrix are greatly weakened. As a small amount of 50 nm-AlN is filled, the amount of aggregation and void is small, and the interaction between AlN and epoxy-matrix can cause the decrease in mobility of epoxy chain. Thus, the T_g increases with increasing a small amount of 50 nm-AlN. Further adding the 50 nm-AlN content, more aggregations of nano-AlN and voids exist in the composite, which greatly improves the mobility of epoxy chain.[28–30] As a result, the T_g decreases at higher 50 nm-AlN content.

Compared with 2.3 μm-AlN, 2.3 μm + 50 nm-AlN-filled composite has smaller T_g because 50 nm-AlN in the composite easily forms the aggregation and causes voids [Figure 7(f)]. But at the same time, its T_g is larger than that of 50 nm-AlN-filled composite owing to the actual amount of 50 nm-AlN in the composite being smaller than that of single 50 nm-AlN-filled composite. Also, the gradual increase in the actual amount of 50 nm-AlN in the composite causes the T_g to first increase then decrease with increasing AlN content. This implies that the effect of 50 nm-AlN in combination of 2.3 μm-AlN and 50 nm-AlN is remarkable and dominative. Owing to the easily agglomerating of 50 nm-AlN and the more voids existing in the composites, the tensile strength and elongation at break of the composites filled with 50 nm-AlN or 2.3 μm + 50 nm-AlN obviously decrease with AlN content above 1.2 vol %. The increased defects, such as aggregations and voids, induce the increase of dielectric dissipation in addition to enhancement in interface dissipation as the 50 nm-AlN content is increased. Thus, the D_f of 50 nm-AlN-filled composite abnormally increases as AlN content above 2.36 vol %.

Figure 7(g,h) shows the SEM images of 27.91 vol % 2.3 μm-AlN and 2.3 + 0.5 μm-AlN-filled composite prepared at low vacuum, respectively. It is revealed that some of the AlN filler have been debonded from the epoxy matrix, indicating the weak adhesion between AlN filler and epoxy matrix. Moreover, microfibrils, which would demonstrate interfacial adhesion, are not observed from the micrographs. This also indicates that the interfacial adhesion between AlN and epoxy matrix is weak. In addition, it can be found that voids increase owing to the existence of more solvent during preparation compared with the composites prepared at high vacuum. It is believed that the obvious degeneration in properties of the composites prepared at low vacuum is related to the more voids and poor interfacial interaction between filler and matrix in the composites. For the thermal conductivity of the 2.3 μm-AlN-filled composite, it slightly increases at low vacuum condition although the more voids should exist in the composite and thus should decrease the thermal conductivity. The reasons for this abnormal increase of thermal conductivity need to be further investigated.

In addition to microstructure, the properties of the composites are also considered to be related to the crosslink density of the epoxy matrix, and thus the infrared absorption spectra of the composites are examined as shown in Figure 8. As shown in Figure 8, the infrared absorptive peaks are similar to all composites. The peak at 710 cm^{-1} is attributed to AlN,[31] and it used as an internal standard. The peaks at 829, 1035, 1182, 1246, and

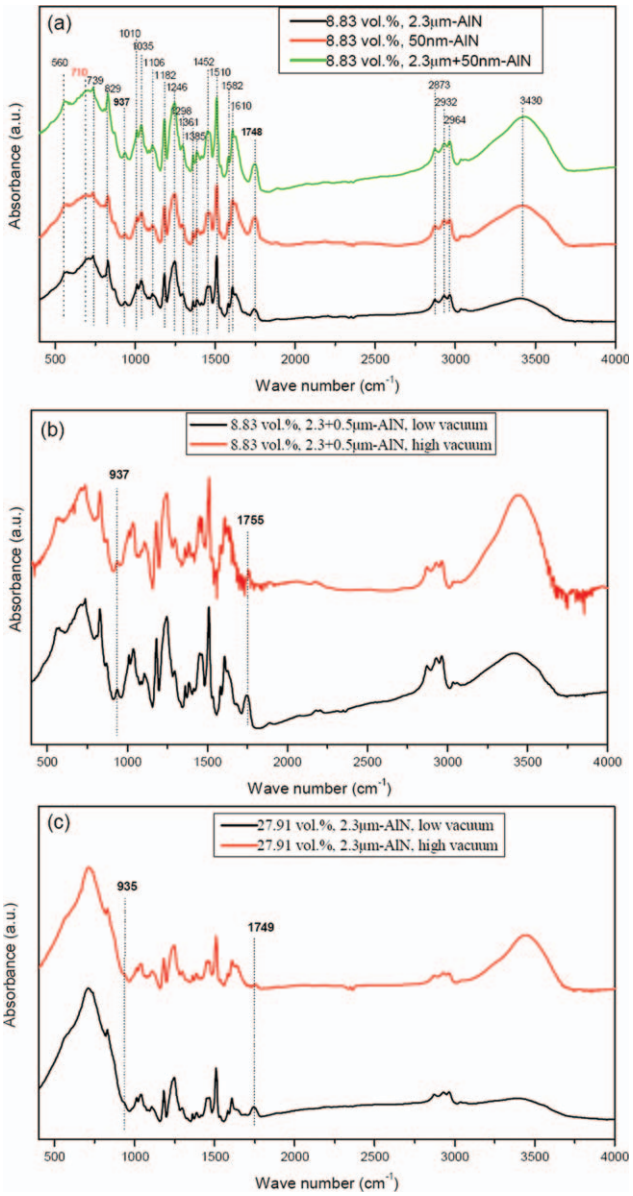

Figure 8. The change of infrared absorption spectra for the composites filled with 8.83 vol % 50 nm-AlN, 2.3 μm-AlN, and 2.3 μm + 50 nm-AlN and prepared at high vacuum condition (a), filled with 8.83 vol % 2.3 + 0.5 μm-AlN and prepared at high and low vacuum conditions (b), and filled with 27.91 vol % 2.3 μm-AlN and prepared at high and low vacuum conditions (c). [Color figure can be viewed in the online issue, which is available at wileyonlinelibrary.com.]

1510 cm^{-1} are the characteristic absorption of DGEBA structure; those at 739, 1010, 1106, 1298, and 1452 cm^{-1} are associated with the diglycidyl ether of tetrabromobisphenol A (DGETBBA); those at 560 and 1582 cm^{-1} are related to DGEBA–DGETBBA.[32,33] The two peaks of 1362 and 1385 cm^{-1} appear simultaneously, indicating the existence of isopropylidene.[32,33] The absorptive peaks near 1298 and 1748 cm^{-1} are owing to the stretching vibration of C—N and carbonyl groups of 2-oxazolidinone, which are formed during the curing of DGEBA.[32,33] The peak near 935 cm^{-1} is originated from epoxide band, which can reflect the curing degree of the epoxy.[18,19]

As shown in Figure 8(a), it is found that the peak intensity of 935 cm^{-1} is increased after adding 50 nm-AlN into composites compared with composite filled with 2.3 μm-AlN at the same preparation condition. As shown in Figure 8(b,c), it is found that peak intensity of 935 cm^{-1} is increased for composites prepared at low vacuum compared with that at high vacuum at the same AlN size and content. Higher peak intensity of 935 cm^{-1} implies that existence of more epoxy, that is more epoxy does not take the crosslinking reaction and thus the crosslink density of epoxy matrix is decreased. The absorptive peaks near 1748 cm^{-1} is attributed to carbonyl groups of 2-oxazolidinone that are formed during the curing of DGEBA, as mentioned above. Thus, the peak intensity of 1748 cm^{-1} should decrease as the peak intensity of 935 cm^{-1} increases. However, both 1748 and 935 cm^{-1} peaks increase when comparing the composites filled with different sized AlN [Figure 8(a)] or prepared at different vacuum conditions [Figure 8(b,c)]. Considering that the solvent used is acetone and functional group of acetone is also carbonyl groups, we presume that the increase in peak intensity of 1748 cm^{-1} may be originated from the acetone dissolving into composite or involving the reaction during curing process. Obviously, more acetone dissolves into the composites or involves the reaction during curing process owing to the increase of viscosity of the system as decreasing AlN size or difficulty of removing solvent at low vacuum conditions. The decrease in crosslink density will subsequently influence the rotational and/or vibrational freedom of the main and/or side chains of epoxy, and thus decreasing T_g and increasing the D_k and D_f for the composites filled with 50 nm-AlN or prepared at low vacuum conditions.[14,19,30,34]

It is worth noting that CTE of the composite decreases and its E increases with increasing 50 nm-AlN content although T_g decreases owing to the weak interaction between AlN and epoxy and decrease of crosslink density of epoxy matrix resulting in removal of epoxy chain. This is because the CTE and E of the composites are related to macroscopic deformation of the composites, which can be hindered by AlN to result in decrease of CTE and increase in E with increasing AlN content. Compared with 2.3 μm-AlN, 50 nm-AlN has a higher surface area, which implies that more interfacial area forms between 50 nm-AlN and the epoxy even if the existence of the aggregation of 50 nm-AlN. Thus, 50 nm-AlN could more effectively restrict the deformation of the epoxy matrix although the interaction of the epoxy and 50 nm-AlN is weak in some regions because of the aggregation of 50 nm-AlN and voids, as discussed previously. As a result, CTE of the 50 nm-AlN-filled composites is lower, and E is higher compared with those of the 2.3 μm-AlN-filled composites.

Finally, it should be pointed out that AlN size and content as well as composite processing conditions also affect the preparation of the composites. As discussed above, the solvent and bubble are difficult to remove and the flowability of the mixture of epoxy and filler is decreased owing to the increase of viscosity of the mixture with increasing the AlN content or decreasing AlN size. Thus, macroscopic voids, caused by poor flowability of the mixture and/or solvent evaporation during curing at high temperature, easily appear at the sample with increasing filler content. In fact, poor moldability of the composites is observed as 50 nm-AlN and 2.3 μm-AlN content increase to 8.83 and 36.74 vol %, respectively, and thus the larger-sized samples for measuring mechanical properties and thermal conductivity cannot be easily obtained. The solvent of acetone can increase the flowability of the mixture of epoxy and filler, and the samples with macroscopic voids free can be obtained occasionally. However, the existence of residual acetone greatly decreases the properties of the composites, as discussed above. In addition, acetone evaporation during curing causes the macroscopic voids in the samples in most cases. Thus, poor vacuum conditions during removal of solvent result in poor moldability of the composites. Obviously, removing the solvent and increasing the flowability of the mixture of epoxy and filler at the same time are important for the preparation of the composites. Decreasing filler content, especially nanometer-sized filler content, can decrease the viscosity of mixture, and thus the moldability of the composites enhances. However, better properties of the composites can be obtained at higher filler content. The studies had indicated that combination of nanometer-sized and micrometer-sized filler can effectively decrease the viscosity and thus the filler content can be increased.[35,36] At the same time, the properties of the composites can be improved when using combination of different sized filler, which had suggested by many researchers.[37,38] On the other hand, the surface treatment of the filler is found to effectively decrease the viscosity of system recently,[39] and the dispersion of nanometer-sized filler can be improved by surface treatment at the same time.[40,41] In a word, the properties of the composites are closely related to their preparation; to control the preparation, selecting the filler size and surface treating should be considered in the further study.

CONCLUSIONS

Basically, it is found that E, D_k, and thermal conductivity increase, whereas CTE and D_f decrease with increasing AlN content; E, D_k, and D_f increase, whereas CTE and T_g decrease with decreasing AlN size. The tensile strength, elongation at break, and T_g of composites exhibit parabolic change with AlN content, and they reach relatively larger values at smaller AlN content with decreasing AlN size. At the same AlN size and content, the composites prepared at low vacuum conditions exhibit poor properties, that is, lower T_g and larger CTE, D_k, and D_f. By analysis of SEM and FTIR, it is thought that AlN size and content as well as processing condition affect the microstructure of the composites and crosslink density of the epoxy, that is more aggregations of AlN and voids easily appear and crosslink density decreases with adding nanometer-sized AlN filler and low vacuum conditions, which results in degeneration of properties of the composites. At the same time, nanometer-sized AlN and low vacuum conditions also affect the removal of solvent and bubble and/or the flowability of the mixture during preparation, and thus result in poor formability of the composites.

ACKNOWLEDGMENTS

This work was supported by the grant from the National Nature Science Foundation of China (Grant No. 50902105) and Research Grants Council of the Hong Kong Special Administrative Region (Project No. PolyU5315/05E).

REFERENCES

1. Lee, G. W.; Park. M.; Kim, J.; Lee, J. I.; Yoon, H. G. *Compos. A Appl. Sci. Manuf.* **2006,** *37*, 727.
2. Yung, K. C.; Wang, J.; Yue, T. M. *Adv. Compos. Mater.* **2006,** *15*, 371.
3. Todd, M. G.; Shi, F. G. *IEEE Trans. Compon. Pack. Technol.* **2003,** *26*, 667.
4. Kim, W.; Bae, J. W.; Choi, I. D.; Kim, Y. S. *Polym. Eng. Sci.* **1999,** *39*, 756.
5. Wong, C. P.; Bollampally, R. S. *J. Appl. Polym. Sci.* **1999,** *74*, 3396.
6. Procter, P.; Solc, J. *IEEE Trans. Compon. Hybrids Manuf. Technol.* **1991,** *14*, 708.
7. Ohashi, M.; Kawakami, S.; Yokogawa, Y.; Lai, G. C. *J. Am. Ceram. Soc.* **2005,** *88*, 2615.
8. Lee, G. W.; Lee, J. I.; Lee, S. S.; Park, M.; Kim, J. *J. Mater. Sci.* **2005,** *40*, 1259.
9. Xu, Y. S.; Chung, D. D. L.; Mroz, C. *Compos. A Appl. Sci. Manuf.* **2001,** *32*, 1749.
10. Bae, J. W.; Kim, W.; Cho, S. H.; Lee, S. H. *J. Mater. Sci.* **2000,** *35*, 5907.
11. Hsieh, C. Y.; Chung, S. L. *J. Appl. Polym. Sci.* **2006,** *102*, 4734.
12. Yu, S. Z.; Hing, P.; Hu, X. *Compos. A Appl. Sci. Manuf.* **2002,** *33*, 289.
13. Yu, S. Z.; Hing, P.; Hu, X. *J. Appl. Phys.* **2000,** *88*, 398.
14. Yung, K. C.; Wu, J.; Yue, T. M.; Xie, C. S. *J. Compos. Mater.* **2006,** *40*, 567.
15. Yung, K. C.; Zhu, B. L.; Wu, J.; Yue, T. M.; Xie, C. S. *J. Polym. Sci. Part B: Polym. Phys.* **2007,** *45*, 1662.
16. Yung, K. C.; Zhu, B. L.; Yue, T. M.; Xie, C. S. *J. Appl. Polym. Sci.* **2010,** *116*, 225.
17. Zhu, B. L.; Ma, J.; Wu, J.; Yung, K. C.; Xie, C. S. *J. Appl. Polym. Sci.* **2010,** *118*, 2754.
18. Hong, S. G.; Wu, C. S. *Thermochim. Acta* **1998,** *316*, 167.
19. Hong, S. G.; Wu, C. S. *J. Therm. Anal. Calorim.* **2000,** *59*, 711.
20. Xu, J. W.; Wong, C. P. *Compos. A Appl. Sci. Manuf.* **2007,** *38*, 13.
21. Zong, L. M.; Kempel, L. C.; Hawley, M. C. *Polymer* **2005,** *46*, 2638.
22. Zhou, Y. X.; Pervin, F.; Rangari, V. K.; Jeelani, S. *Mater. Sci. Eng. A Struct. Mater. Prop. Microstruct. Process.* **2006,** *426*, 221.
23. Qi, B.; Zhang, Q. X.; Bannister, M.; Mai, Y. W. *Compos. Struct.* **2006,** *75*, 514.
24. Goyal, R. K.; Tiwari, A. N.; Mulik, U. P.; Negi, Y. S. *Compos. A Appl. Sci. Manuf.* **2007,** *38*, 516.
25. Goyanes, S. N.; Konig, P. G.; Marconi, J. D. *J. Appl. Polym. Sci.* **2003,** *88*, 883.
26. Choi, Y. K.; Sugimoto, K.; Song, S. M.; Gotoh, Y.; Ohkoshi, Y.; Endo, M. *Carbon* **2005,** *43*, 2199.
27. Xu, J. W.; Moon, K. S.; Tison, C.; Wong, C. P. *IEEE Trans. Adv. Pack.* **2006,** *29*, 295.
28. Ash, B. J.; Siegel, R. W.; Schadler, L. S. *J. Polym. Sci. Part B: Polym. Phys.* **2004,** *42*, 4371.
29. Miyagawa, H.; Drzal, L. T. *Polymer* **2004,** *45*, 5163.
30. Preghenella, M.; Pegoretti, A.; Migliaresi, C. *Polymer* **2005,** *46*, 12065.
31. Zhang, Y. H.; Binner, J. *J. Mater. Sci. Lett.* **2002,** *21*, 803.
32. Liu, G.; Liu, H.; Liu, Y.; He, S. Y. *Polym. Degrad. Stab.* **2011,** *96*, 732.
33. Luda, M. P.; Balabanovich, A. I.; Zanetti, M.; Guaratto, D. *Polym. Degrad. Stab.* **2007,** *92*, 1088.
34. Bandyopadhyay, A.; Valavala, P. K.; Clancy, T. C.; Wise, K. E.; Odegard, G. M. *Polymer* **2011,** *52*, 2445.
35. Greenwood, R.; Luckham, P. F.; Gregory, T. J. *Colloid Interface Sci.* **1997,** *191*, 11.
36. Wang, Q.; Gao, W.; Xie, Z .M. *J. Appl. Polym. Sci.* **2003,** *89*, 2397.
37. Kwon, S. C.; Adachi, T.; Araki, W.; Yamaji, A. *Acta Mater.* **2006,** *54*, 3369.
38. Sanada, K.; Tada, Y.; Shindo, Y. *Compos. A Appl. Sci. Manuf.* **2009,** *40*, 724.
39. Lee, E. S.; Lee, S. M.; Shanefield, D. J.; Cannon, W. R. *J. Am. Ceram. Soc.* **2008,** *91*, 1169.
40. Lee, E. S.; Lee, S. M.; Cannon, W. R.; Shanefield, D. J. *Colloid Surf. A* **2008,** *316*, 95.
41. Jesionowski, T.; Bula, K.; Janiszewski, J.; Jurga, J. *Compos. Interface* **2003,** *10*, 225.